HHS Public Access

Author manuscript

Oncogene. Author manuscript; available in PMC 2016 March 03.

Published in final edited form as:

Oncogene. 2015 September 3; 34(36): 4777–4790. doi:10.1038/onc.2015.224.

A new role of SNAI2 in post-lactational involution of the mammary gland links it to luminal breast cancer development

Sonia Castillo-Lluva[1,2,*], **Lourdes Hontecillas-Prieto**[1,2,*,&], **Adrián Blanco-Gómez**[1,2,$], **María del Mar Sáez-Freire**[1,2,$], **Begoña García-Cenador**[2,3], **Javier García-Criado**[2,3], **Martín Pérez-Andrés**[1,2,4], **Alberto Orfao de Matos**[1,2,4], **Marta Cañamero**[5], **Jian-Hua Mao**[6], **Thomas Gridley**[7], **Andrés Castellanos-Martín**[1,2,#,¶], and **Jesús Pérez-Losada**[1,2,#]

[1]Instituto de Biología Molecular y Celular del Cáncer (IBMCC). Universidad de Salamanca/CSIC. Salamanca. Spain

[2]Instituto de Investigación Biomédica de Salamanca (IBSAL). Hospital Universitario de Salamanca. Salamanca. Spain

[3]Departamento de Cirugía. Universidad de Salamanca. Salamanca. Spain

[4]Unidad de Citometría de flujo. Universidad de Salamanca. IBSAL. Salamanca. Spain

[5]Centro Nacional de Investigaciones Oncológicas (CNIO). Madrid. Spain

[6]Life Sciences Division. Lawrence Berkeley National Laboratory (LBNL). University of California. Berkeley. CA 94720. Berkeley. CA. USA

[7]Center for Molecular Medicine. Maine Medical Center Research Institute. Scarborough, ME, USA

Abstract

Breast cancer is a major cause of mortality in women. The transcription factor SNAI2 has been implicated in the pathogenesis of several types of cancer, including breast cancer of basal origin. Here we show that SNAI2 is also important in the development of breast cancer of luminal origin in *MMTV-ErbB2* mice. SNAI2 deficiency leads to longer latency and fewer luminal tumors, both of these being characteristics of pre-tumoral origin. These effects were associated with reduced proliferation and a decreased ability to generate mammospheres in normal mammary glands. However, the capacity to metastasize was not modified. Under conditions of increased ERBB2 oncogenic activity after pregnancy plus SNAI2 deficiency, both pretumoral defects-latency and tumor load- were compensated. However, the incidence of lung metastases was dramatically

Full name, mailing address, phone and fax number, and email address of the corresponding authors: Dr. A. Castellanos-Martín (andres.castellanos@irbbarcelona.org), and Jesús Pérez Losada (jperezlosada@usal.es). Phone: 34-923-294807. FAX: 34-923-294813.
*Equal contribution as first authors, and listed in alphabetical order of surnames.
$Equal contribution as second authors, and listed in alphabetical order of surnames.
#Equal contribution as senior authors.
&Current address: Departamento de Patología Molecular. Instituto de Biomedicina de Sevilla (IBiS). Sevilla. Spain.
¶Current address: Institute for Research in Biomedicine (IRB). Barcelona. Spain.

Conflicts of Interest: The authors declare no conflict of interest.

"Supplementary Information accompanies the paper on the Oncogene website (http://www.nature.com/onc)"

reduced. Furthermore, SNAI2 was required for proper post-lactational involution of the breast. At three days post-lactational involution, the mammary glands of *Snai2*-deficient mice exhibited lower levels of pSTAT3 and higher levels pAKT1, resulting in decreased apoptosis. The presence of abundant non-involuted ducts was still present at 30 days post-lactation, with a greater number of residual ERBB2+ cells. These results suggest that this defect in involution leads to an increase in the number of susceptible target cells for transformation, to the recovery of the capacity to generate mammospheres, and to an increase in the number of tumors. Our work demonstrates the participation of SNAI2 in the pathogenesis of luminal breast cancer, and reveals an unexpected connection between the processes of post-lactational involution and breast tumorigenesis in *Snai2*-null mutant mice.

Keywords

SNAI2; ERBB2; Luminal breast cancer; post-lactational involution

Introduction

Breast cancer is one of the leading causes of death among women worldwide. It is a complex and heterogeneous disease with substantial variations in its molecular and clinical characteristics.[1] ERBB2/NEU/HER2 (henceforth ERBB2)-positive breast cancers constitute 20-30% of all mammary gland tumors, and ERBB2 amplification and overexpression are markers of poor prognosis.[2] Breast cancer evolution is characterized by different stages of progression; the final one is distant metastasis, responsible for the poor survival seen in this disease.

The transcription factor SNAI2/SLUG is involved in the process of epithelial to mesenchymal transition (EMT) by repressing E-cadherin expression.[3, 4] SNAI2 has been associated with tumor invasion and metastasis and the poor prognosis of several tumor types, including breast carcinoma.[3] Furthermore, SNAI2 has additional cellular functions such as the inhibition of apoptosis,[5-7] the regulation of cell movement, adhesion, proliferation[8] and stem-cell properties,[9, 10] all of them important in tumor pathogenesis and evolution.[11] SNAI2 has also been linked to early differentiation and morphogenesis in several tissue types.[4]

The importance of SNAI2 in the determination of the basal phenotype in breast cancer of both sporadic and *BRCA1*-mutated origins has been demonstrated previously.[12, 13] However, SNAI2 is rarely expressed in luminal breast cancer cells[14] (Supplementary Figure S1a). In the mammary gland, SNAI2 is expressed in normal breast tissue and is localized in the proliferative basal compartment during mammary gland morphogenesis,[9, 15] but it is not known whether SNAI2 might play a role in the development of luminal tumors. To address this point, we studied the participation of SNAI2 in the development of breast cancer in *MMTV-ErbB2* mice,[16] which develop breast tumors of the luminal phenotype.[17] Here, we demonstrate that SNAI2 is important for the development of luminal tumors induced by ERBB2. In particular, SNAI2 deficiency protected mice from breast tumorigenesis, led to an extended tumor latency and overall survival with fewer tumors, with only a very weak effect

on dissemination. Since tumor latency and yield have their origin in pre-tumoral stages, this demonstrates the participation of SNAI2 in early phases of breast cancer development of luminal origin. Interestingly, in response to an increased expression of the ERBB2 transgene during pregnancy, this protective effect observed in the absence of SNAI2 disappeared, but the defect in the dissemination of metastases was exacerbated. We also report results demonstrating the importance of SNAI2 for proper mammary gland involution, and a connection between this process and breast tumorigenesis in *Snai2* knockout (KO)$^{ERBB2+}$ mice.

Results

SNAI2 deficiency alters the susceptibility and evolution of breast cancer of luminal origin induced by ERBB2

To determine whether SNAI2 was involved in the susceptibility to and evolution of luminal breast cancer, we crossed B6;129S1-*Snai2*^{tm2Grid}/J[18] with FVB/N-Tg(MMTVneu)202Mul/J transgenic mice, which develop luminal tumors.[16, 17] Thus, we established a *Snai2*-deficient line that overexpresses the ERBB2 protooncogene (henceforth *Snai2* KO^{ERBB2+}). To avoid the C57BL/6 resistance effect in breast cancer development,[19-21] F1 transgene-positive/ *Snai2*-deficient males were backcrossed with FVB females to obtain the F4 generation with more than 90% FVB genetic background,[22] as described in the Methods section. To better evaluate the effect of SNAI2 in the different features of breast cancer, we differentiated several pathophenotypes in the disease. We evaluated latency, disease duration and lifespan, and tumor traits of progression, such as the number of tumors, local growth and metastases. We observed that *Snai2* KO^{ERBB2+} mice had a longer tumor latency than *Snai2* WT^{ERBB2+} animals (median of 54.1 versus 47.7 weeks, respectively), with no significant differences in the duration of the disease, thus leading to longer life-spans (Figures 1a-c and Table 1). In addition, *Snai2* KO^{ERBB2+} mice developed significantly fewer tumors than *Snai2* WT^{ERBB2+} mice, with no differences in local tumor growth (Figure 1d and Table 1). Because SNAI2 has been implicated in metastasis,[4, 5, 8, 23] we compared the frequency of metastasis in the *Snai2* WT^{ERBB2+} and *Snai2* KO^{ERBB2+} mice. Unexpectedly, we did not find differences in the median and incidence of metastasis (62.5% of *Snai2* WT^{ERBB2+} mice developed metastasis versus 50.0% of *Snai2* KO^{ERBB2+} mice). No differences were seen in the multiplicity of metastatic impacts in the lungs either (i.e. the percentage of mice already having metastasis with two or more impacts) (Figures 1e and 1f, and Table 1).

Interestingly, SNAI2 was expressed in the mammary gland but not in the bulk of the tumor (Figure 1g and Supplementary Figure S1b). The breast tumors generated in *Snai2* KO^{ERBB2+} mice were ER-negative, PR-negative, and ERBB2-positive. They were positive for the luminal cytokeratins CK8 and CK18 and negative for the basal cytokeratin CK6. In addition, there were no significant differences in the expression levels of several luminal markers, such as Gata3, Sox9, and CK18, between tumors from the *Snai2* KO^{ERBB2+} and *Snai2* WT^{ERBB2+} mice (Supplementary Figures S1c-g). To gain further insight into the characterization of ERBB2-positive tumors generated in the absence of *Snai2*, we evaluated the distribution of the epithelial cell hierarchy in the tumors. The bulk of the epithelial population in the ERBB2+ tumors was formed by CD24^{hi}CD29^{lo} luminal cells in agreement

with previous studies,[24] and there were no differences in the luminal, basal ($CD24^{lo}CD29^{hi}$) and stem-cell-enriched populations ($CD24^{lo}CD49f^{hi}CD29^{hi}$) between tumors from *Snai2* WT^{ERBB2+} and *Snai2* KO^{ERBB2+} mice (Figure 1h). These results suggested that *Snai2* KO^{ERBB2+} mice develop tumors of luminal origin, as has been reported previously for *Snai2* WT^{ERBB2+} mice.[17]

Pregnancy recovers local breast tumorigenesis in *Snai2* KO^{ERBB2+} mice but increases the proportion of metastasis-free mice

It has been reported that pregnancy increases the expression of the *ErbB2* protooncogene, driven by the *MMTV* promoter, resulting in a more aggressive disease.[16, 25] We therefore wondered to what extent SNAI2 would be necessary for luminal breast cancer development generated under increasing oncogenic activity of ERBB2 after pregnancy. As expected, we observed an exacerbation of the disease in both *Snai2* WT^{ERBB2+} and *Snai2* KO^{ERBB2+} parous mice, resulting in a statistically significant decrease in latency and lifespan, but with no modification in the duration of the disease (Supplementary Figures S2a-f, and Table 1).

In the *MMTV-ErbB2* transgenic mice, these effects of SNAI2 deficiency on luminal tumor development were compensated after pregnancy. Parous *Snai2* WT^{ERBB2+} mice displayed a significantly shorter latency than their nulliparous counterparts, as reported,[16, 26] but no significant modifications in the number of tumors were observed (Supplementary Figures S2a and S2g). By contrast, parous *Snai2* KO^{ERBB2+} mice showed both a shorter latency and a significant increase in the number of tumors with respect to their nulliparous analogues (Supplementary Figures S2b and S2h). In fact, the effect on both the latency and tumor numbers in parous *Snai2* KO^{ERBB2+} mice was more evident than in their parous wild-type equivalents (Figure 2a). This meant that the differences in latency and tumor number previously observed between nulliparous *Snai2* WT^{ERBB2+} and nulliparous *Snai2* KO^{ERBB2+} mice had disappeared in their parous counterparts (Figures 2b, 2d and 2e, and Table 1). However, the induction of ERBB2 by pregnancy did not modify the duration of the disease (Figure 2c and Supplementary Figures S2e and S2f, and Table 1). This is in agreement with the observation that, because metastases are well tolerated in this model, local tumor growth is the main pathophenotype that determines the duration of the disease, and latency is the one that mainly determines lifespan (Table 1).[27]

Regarding tumor dissemination, parity significantly increased the incidence and multiplicity of metastases in *Snai2* WT^{ERBB2} mice with respect to their nulliparous counterparts (Table 1). The absence of SNAI2 increased the percentage of metastasis-free mice under increasing ERBB2 oncogenic activity. Thus, the incidence of metastasis in parous *Snai2* KO^{ERBB2+} mice was significantly lower than in parous *Snai2* WT^{ERBB2+} animals (61% versus 90.47%, respectively; $P = 0.0276$) without modification of multiplicity (Figures 2f and 2g, and Table 1).

Moreover, there were no significant differences in ERBB2 expression between tumors from nulliparous and parous mice of both the WT and KO *Snai2* genotypes (Supplementary Figures S1c and S2i-k). This is in agreement with the fact that there were no significant differences in the local growth speed, proliferation and apoptosis between tumors from nulliparous and parous *Snai2* WT^{ERBB2+} and *Snai2* KO^{ERBB2+} mice (Supplementary

Figures S2l and S2m). Furthermore, we analyzed the tumor epithelial cell hierarchy from parous mice. Again, the bulk of the population was formed by epithelial cells without significant differences between tumors from parous *Snai2* WT^{ERBB2+} and parous *Snai2* KO^{ERBB2+} mice. Surprisingly, we saw a slight but significant difference in the basal ($CD24^{lo}CD29^{hi}$) and the stem-cell-enriched ($CD24^{lo}CD49f^{hi}CD29^{hi}$) subpopulations in favor of the tumors from the *Snai2* KO^{ERBB2+} mice after pregnancy conditions (Figures 2h and 2i).

Mammary glands from nulliparous *Snai2* KO^{ERBB2+} mice show defects in cellular turnover

Since the *Snai2* deficiency modified tumor characteristics originating in pretumoral stages, such as latency and the number of tumors, we evaluated the morphology of mammary glands from adult nulliparous mice at two months of age. Normally, the extension of fat pad filled by ducts is used as a criterion for assessing the ability of mammary epithelial cells to undergo ductal growth.[28] The fat pads of the *Snai2* KO^{ERBB2+} mice were completely filled by ducts, similar to wild-type mice (Figure 3a), but the ducts in the glands of the *Snai2* KO^{ERBB2+} female mice were characterized by a reduced presence of side-branching as compared with their *Snai2* WT^{ERBB2+} counterparts (Figures 3b), as recently reported in non-transgenic *Snai2* KO^{WT} mice.[9] However, we did not find differences in the number of terminal end-buds (Supplementary Figures S3a and S3b). Previously, an impairment in ductal growth has been reported in *Snai2* WT^{ERBB2+} transgenic mice with respect to their control *Snai2* WT^{WT} non-transgenic counterparts,[29] as reflected by a shorter average ductal length (defined as the distance from the center of the lymph node to the leading edge of the gland); this shortening was also confirmed here ($P = 0.018$) (Figure 3c). In addition, mice that overexpressed ERBB2 in the context of *Snai2* deficiency showed a similar shortening of average ductal length with respect *Snai2* WT^{WT} non-transgenic mice, but there was only a statistical trend ($P = 0.083$) (Figure 3c). Furthermore, there were no significant differences in the expression levels of several markers of luminal lineage described previously,[9] such as the progesterone receptor (*PR), Gata3* and *Ck18*, between mammary glands from *Snai2* KO^{ERBB2+} and *Snai2* WT^{ERBB2+} mice (Supplementary Figure S3c). In addition, transgenic expression of *ErbB2* in the mammary gland did not modify the SNAI2 localization already described in the basal compartment[9] (Supplementary Figure S3d).

Latency is the time required for the initiated target cells to acquire the fully transformed phenotype, which is related to the baseline proliferation of a tissue. Thus, the higher the proliferation itself, or in the presence of promoting agents, the easier it becomes for the cells to acquire new secondary oncogenic events and the shorter the latency time.[30] In light of this, we analyzed cellular turnover in terms of the rate of cell proliferation and apoptosis in histologic sections of mammary glands from *Snai2* WT^{ERBB2+} and *Snai2* KO^{ERBB2+} mice. Interestingly, according to Ki67 staining (Figure 3d) mice deficient in *Snai2* showed a significantly decreased proliferation in the mammary epithelia of nulliparous mice and lower levels of CYCLIN D1 (Figure 3e). Surprisingly, nulliparous *Snai2* KO^{ERBB2+} mice showed discretely but significantly lower levels of baseline apoptosis (active CASPASE-3 staining) than their wild-type counterparts (Figure 3f).

Nulliparous *Snai2* KO^{ERBB2+} mice have defects in stem-cell populations in the mammary gland

Mammary stem cells have been implicated in the origin of breast cancer,[31] and the number of stem cells is reflected in the number of mammospheres generated *in vitro*.[32] Moreover, SNAI2 participates in the stem-cell biology of the mammary gland.[9, 10, 33] Because latency and tumor numbers are both traits of breast cancer determined in pretumoral stages, we evaluated the generation of mammospheres in the mammary glands of nulliparous *Snai2* KO^{ERBB2+} mice. *Snai2* KO^{ERBB2+} mice had a diminished capacity to generate mammospheres, but these maintained their ability to expand *in vitro* (Figures 3g and h). Interestingly, the expression of SNAI2 in mammospheres was enriched in comparison with its levels of expression in mammary gland epithelial cells (Figure 3i), in agreement with the role of SNAI2 in mammary stem-cell biology.[9, 10, 34] Nevertheless, we did not observe differences in mammosphere formation in *Snai2* KO^{WT} non-transgenic mice (Supplementary Figure S3e).

Since normal mammary glands from *Snai2* KO^{ERBB2+} mice generated fewer mammospheres than nulliparous *Snai2* WT^{ERBB2+} mice, suggesting that the nulliparous *Snai2* KO^{ERBB2+} animals would have fewer target mammary stem cells susceptible to transformation than *Snai2* WT^{ERBB2+} mice, we used flow cytometry to evaluate the number of stem cells and other subpopulations in the mammary glands of the nulliparous mice. We did not observe clear differences in the percentage of the CD24^{+}/CD49f^{hi}/CD29^{hi} subpopulations identified as mammary stem cells in the literature[31, 35] (Supplementary Table S1). Thus, in the *Snai2* KO^{ERBB2+} mice we evaluated other cell subpopulations described in the mammary gland from *Snai2* WT^{ERBB2+} transgenic mice.[24, 36-39] The nulliparous *Snai2* KO^{ERBB2+} mice had no differences in the population of Sca1^{pos} cells, reported to be enriched for functional stem/progenitor cells with increased regenerative potential,[36, 37] and we also failed to find differences in the CD24^{+}Sca1^{+} subpopulation, specifically described to have self-renewal capability in *Snai2* WT^{ERBB2+} mice.[24] Moreover, neither did we find differences in the CD49f^{+}CD61^{hi} population described as being enriched in tumor-initiating cells in *Snai2* WT^{ERBB2+} transgenic mice.[38] Finally, we did not find differences in the number of luminal progenitors CD24^{hi}CD29^{med} with self-renewal capability.[39] EpCAM has recently been described as a better marker that permits greater resolution of the epithelial mammary gland subpopulations in the mouse.[40, 41] Thus, we re-analyzed all these populations with the anti-EpCAM antibody, but failed to find any difference either (Supplementary Table S1). We were also unable to demonstrate differences in the mammary glands from nulliparous *Snai2* KO^{ERBB2+} mice in luminal cells in spite of the function of SNAI2 described in the luminal and stem-cell compartments[10, 12, 33] (Supplementary Table S1).

All the data presented above suggested that there seem to be no-differences in the number of putative targets of tumors in *MMTV-ErbB2* mice in the absence of *Snai2*. Nevertheless, the fact that we observed a diminished capability in mammosphere production (Figure 3g) suggests that there is a functional defect in self-renewal capability in MSCs from *Snai2* KO^{ERBB2+} mice. Moreover, because we observed that the propagating capability of

mammospheres was normal (Figure 3h), this suggests the defect in MSCs would be non-cell-autonomous due to other compartments, probably in the niche.

The defect in mammosphere yield in nulliparous *Snai2* KO^{ERBB2+} mice is compensated after pregnancy

Since the defect in latency and number of tumors disappeared after pregnancy, we assessed the cellular turnover and the ability to generate mammospheres in parous mice. To evaluate the behavior of the mammary gland after the most active phases of involution, we carried out this study at thirty days after the end of lactation. Under these conditions, and despite a higher epithelial cellularity (addressed in the next section), there was also a reduced proliferation in the mammary glands of parous *Snai2* KO^{ERBB2+} mice (Figure 4a), associated with lower levels of CYCLIN D1 (Figure 4b). Parous *Snai2* KO^{ERBB2+} mice also exhibited less apoptosis in the mammary glands, but this was not statistically significant (Figure 4c).

In addition, the generation of mammospheres by parous *Snai2* WT^{ERBB2+} and parous *Snai2* KO^{ERBB2+} mice was equivalent, indicating similar stem-cell activity in the mammary glands (Figure 4d and Supplementary Figure S3f). This is consistent with the fact that no statistical differences were observed in the number of tumors generated between parous *Snai2* WT^{ERBB2+} and parous *Snai2* KO^{ERBB2+} mice (Figure 2e). Neither were there any differences between the number of mammospheres generated by nulliparous *Snai2* WT^{ERBB2+} mice versus parous *Snai2* WT^{ERBB2+} mice (Supplementary Figure S3g), and again this was correlated with the absence of differences in the number of tumors generated (Supplementary Figure S2g). Increased mammosphere production was only seen in the parous *Snai2* KO^{ERBB2+} mice (Supplementary Figure S3h), which, as indicated, could explain the increase in tumor susceptibility observed in these rodents as compared to nulliparous *Snai2* KO^{ERBB2+} mice (Supplementary Figure S2h).

Parous *Snai2* KO^{ERBB2+} mice display a delay in mammary gland involution

We next evaluated the histology of the mammary glands of parous mice. The observation of the mammary glands of *Snai2* KO^{ERBB2+} mice at thirty days post-lactation revealed the presence of more residual ducts with proteinaceous material inside than in the mammary glands from the wild-type mice, suggesting a delay in involution (Figures 5a and 5b). Mammary gland involution is a complex process in which the lactating gland returns to a previous morphologically pre-pregnant state. This process is characterized by substantial apoptosis in epithelial cells, the regeneration of adipose mammary tissue, and global tissue remodeling.[42] Although remains of the lactating mammary gland can be found as vestiges in normal involuted breast tissue,[43] the mammary glands of *Snai2* KO^{ERBB2+} mice showed vestiges much more frequently than the *Snai2* WT^{ERBB2+} glands (Figures 5a and 5b).

In light of the foregoing, we evaluated the delay in the involution of the mammary gland in greater detail. We first assessed the global morphology of the mammary gland in the *Snai2* KO^{ERBB2+} mice immediately after lactation, at three days of involution. In whole-mount evaluations, we observed smaller hypoplastic glands at necropsy (Supplementary Figure S4a), with a less dense branching pattern. This was particularly evident at the periphery of

the gland, indicating a less hyperplastic mammary gland. This permitted the lymph node to be visualized in 6 out of 11 mammary glands, whereas the node was visible only in 1 out of 10 mammary glands from independent parous *Snai2* WT^{ERBB2+} female mice (Supplementary Figures S4b and S4c). This result is in agreement with a recent report that suggested that *Snai2* deficiency affects mammary gland development during pregnancy.[34] Despite this, as indicated above, in the mammary glands of *Snai2* KO^{ERBB2+} mice we observed more residual ducts than in the mammary glands from the wild-type mice due to a delay in involution (Figures 5a and 5b).

In addition, the mammary glands of the *Snai2* KO^{ERBB2+} mice also showed histopathological features of delayed involution at three days post-lactation, exhibiting fewer apoptotic cells inside, as well as a lower overall staining of active-CASPASE-3 as compared with their wild-type counterparts (Figures 5c-f). Importantly, the delay in the involution process was already present in non-transgenic parous *Snai2* KO^{WT} mice (Supplementary Figures S5a-c), indicating that SNAI2 was necessary for normal mammary gland involution. This is in agreement with the broad expression of SNAI2 at three days of post-lactational involution in the mammary gland observed here (Figure 5d).

SNAI2 is required for STAT3 activation during post-lactational involution of the mammary gland

To study the molecular mechanism that led to a defect in the involution of the mammary gland under *Snai2* deficiency, we studied the levels of some targets primarily involved in the involution process. Activation of STAT3 is essential for triggering post-lactational involution; pSTAT3 in turn interferes with the PI3K pathway, leading to lower levels of pAKT1 and apoptosis in mammary epithelial cells.[44-46] Here we show that mammary glands from parous *Snai2* KO^{ERBB2+} mice had significantly lower levels of pSTAT3(Y705), together with higher levels of pAKT1(S473) than their wild-type counterparts at three days of post-lactational involution. This could explain the delay in mammary gland involution in the *Snai2* KO^{ERBB2+} mice (Figures 5g-i). The delay in the involution process already present in non-transgenic parous *Snai2* KO^{WT} mice also showed the same defect in STAT3 activation, indicating that this was specifically due to the SNAI2 deficiency (Supplementary Figures S5d and S5e). We did not observe differences in the baseline levels of pAKT1 or pSTAT3 in the mammary glands of nulliparous mice (Supplementary Figures S6a and S6b).

We observed that the defect in mammary gland involution in parous *Snai2* KO^{ERBB2+} mice was still detectable at thirty days post-lactation (Figure 5a). Accordingly, we analyzed the ERBB2 status and found that there was more ERBB2 expression, and more ERBB2+ cells at 30 days post-involution in parous *Snai2* KO^{ERBB2+} mice, probably as consequence of a defect in elimination during the involution process (Figures 6a and 6b). These results could explain the later increased latency and tumor numbers. Furthermore, the highest levels of pAKT1(S473) were also detected at 30 days post-involution, together with abnormally high levels of pSTAT3 in the mammary glands of parous *Snai2* KO^{ERBB2+} mice (Figure 6c). The activation of both AKT1 and STAT3 at 30 days is probably a consequence of the presence of more ERBB2+ cells. Indeed, STAT3 expression is correlated with ERBB2 expression in human tumors.[47, 48]

To further study the influence of SNAI2 levels in AKT1 and STAT3 activation, we used HC11 cells, a clonal epithelial cell line derived from a mid-pregnant mouse mammary gland capable of lactogenic differentiation under hormonal stimuli.[49] In this cell line, both prolactin and progesterone were able to induce the phosphorylation of AKT and increase the levels of SNAI2 (Figure 6d and Supplementary Figure S6d). Interestingly, after down-regulation of *Snai2* by shRNA, the activation of AKT and the decrease in pSTAT3 were more evident (Figure 6d and Supplementary Figures S6c and S6d). Furthermore, this effect was also seen even in the absence of prolactin (Supplementary Figure S6c), suggesting that the downregulation of *Snai2* would be sufficient to raise pAKT1(S473) and reduce pSTAT3(Y705) levels. In conclusion, SNAI2 participates in mammary gland involution, helping to activate STAT3 and to inhibit pAKT1. However, the mechanism by which SNAI2 exerts these effects remains unknown.

Snai2 deficiency modifies AKT1 levels in tumors from *Snai2* KO^{ERBB2+} mice through a non-cell autonomous mechanism

Since the *Snai2* deficiency modified the levels of activated STAT3 and AKT1 in the mammary gland, we wondered whether the status of these molecules in the tumors was affected. Interestingly, tumors from parous *Snai2* KO^{ERBB2+} mice showed significantly higher total and phosphorylated levels of AKT1 than tumors from parous *Snai2* WT^{ERBB2+} animals, which could contribute to increasing their relative local aggressiveness and the lower capacity to disseminate.[50, 51] However, we did not see differences in the levels of activated STAT3 (Figures 6e and 6f). Since SNAI2 is not expressed in tumors from *Snai2* WT^{ERBB2+} mice (Figure 1g and Supplementary Figure S1b), this effect on AKT1 levels would be exerted by a non-cell autonomous mechanism. In this sense, a recent report has described a non-cell autonomous effect of SNAI2 in skin cancer progression by promoting the recruitment of myeloid cells.[52] Accordingly, we evaluated myeloid infiltration in breast tumors and we did not see differences between the wild-type and KO mice or between nulliparous and parous mice (Supplementary Figure S6e). Thus, other studies will be needed to clarify the non-cell autonomous effect of SNAI2 deficiency in breast cancer development.

Discussion

In this work we found that *Snai2* KO^{ERBB2+} mice were partially protected from breast tumorigenesis, exhibited an extended latency and therefore lifespan, and had fewer tumors than their *Snai2* WT^{ERBB2+} counterparts. Since both disease pathophenotypes have their origin in pretumoral stages, and because SNAI2 is expressed in the mammary gland but not in the bulk of the tumor (Figure 1g and Supplementary Figure 1b), these results demonstrate the participation of SNAI2 in the early stages of luminal breast cancer development. Surprisingly, in this model of luminal breast cancer, *Snai2* deficiency did not affect the metastatic capacity in these mice.

The increased oncogenic activity of ERBB2 after pregnancy compensated the lower local tumor susceptibility previously demonstrated in nulliparous *Snai2* KO^{ERBB2+} mice regarding tumor latency and the number of tumors; by contrast, it exacerbated the defect in metastatic capacity. These results suggest that a complete inhibition of SNAI2 (e.g. a

pharmacological inhibition) could significantly raise the incidence of metastasis-free individuals in luminal breast cancer. This effect of SNAI2 deficiency on luminal tumor dissemination is in agreement with the fact that a minority of cells inside luminal tumors express basal epithelial genes, and proves that targeting the basal invasive program in luminal tumors could limit metastatic progression.[53] However, we were unable to detect SNAI2 expression in the invasion front either (Supplementary Figure S1b).

Mice deficient in *Snai2* showed a significantly decreased proliferation in the mammary epithelium of nulliparous mice. It has been reported that SNAI2 could be located downstream of ERBB2 in breast cancer cells and could contribute to ERBB2 tumorigenesis.[54] Thus, the absence of SNAI2 might contribute directly to reducing ERBB2 signaling. However, this low proliferation has also been reported in wound healing in *Snai2* KO mice without the ERBB2 transgene,[55] indicating that this low proliferation could affect other tissues without the influence of ERBB2, at least *in vivo*. This effect of *Snai2* deficiency on a lower proliferation rate could be explained in terms of the lower levels of CYCLIN D1 observed here (Figure 3e), in agreement with a previous report that SNAI2 increases CYCLIN D1 levels by inhibiting its ubiquitination.[56] Moreover, CYCLIN D1 is necessary for tumor development in *MMTV-ERBB2* transgenic mice.[57, 58] It is possible that the low baseline proliferation in mammary glands under *Snai2*-deficient conditions would hinder the acquisition of secondary events for the complete transformation of the target cells already initiated by the first oncogenic event (i.e. the *ErbB2* transgene), leading to longer tumor latency.[30, 59] Despite the function of SNAI2 as an inhibitor of apoptosis,[5, 60] nulliparous *Snai2* KO^{ERBB2+} mice showed lower levels of baseline apoptosis than their wild-type counterparts (Figure 3f), in agreement with the effect of *Snai2* deficiency on the skin observed in a recent report.[55]

Interestingly, the nulliparous *Snai2* KO^{ERBB2+} mice showed a lower capacity to generate mammospheres, but these maintained their ability to expand *in vitro*, suggesting a smaller number of functional stem cells *in vivo* but a normal propagation capacity *ex vivo* (Figures 3g and 3h). Thus, we cannot exclude the possibility of the existence of an extrinsic effect of *Snai2* deficiency through other compartments, such as the local niche where stem cells reside. We did not observe differences in mammosphere formation in *Snai2* KO^{WT} non-transgenic mice (Supplementary Figure S3e), which is partially in agreement with a recent report[9] describing some differences in what the authors referred to as microspheres. Thus, the differences in the mammosphere yield observed here in *Snai2* KO mice were only present in the context of ERBB2 overexpression. In this sense, ERBB2 has also been related to mammosphere formation and stem-cell expansion in mice.[61-64] In addition, CYCLIN D1 is required for the self-renewal of mammary stem cells, which are targets of *MMTV-ErbB2* tumorigenesis.[65] It is possible that the observed defect in CYCLIN D1 (Figure 3e) could contribute to the lower mammosphere yield in nulliparous *Snai2* KO^{ERBB2+} mice. Finally, lower numbers of mammospheres and cancer-initiating cells have been described in *MMTV-ErbB2* mice deficient in IKK-alpha, these animals also showing a reduction in mammary tumor incidence and multiplicity.[64] In conclusion, we found a positive association between the number of mammospheres, and therefore functional mammary stem cells, and the number of tumors originating in the *ErbB2* transgenic mice. Furthermore, in response to

pregnancy the *Snai2* KO^{ERBB2+} mice compensated the defect in the number of mammospheres observed in their nulliparous counterparts. It is possible that the defect in CYCLIN D1 (Figures 3e and 4b) could contribute to the lower mammosphere yield in nulliparous *Snai2* KO^{ERBB2+} mice but that it could somehow be compensated in parous *Snai2* KO $^{ERBB2+}$ mice.

We later observed that SNAI2 was necessary for normal mammary gland involution. Here again, the lower apoptosis observed during the involution process in *Snai2* KO mice is paradoxical, considering the function described for SNAI2 as an inhibitor of apoptosis in other systems.[5, 11, 60] The relative expansion of mammospheres, and hence mammary stem cells in parous *Snai2* KO^{ERBB2} mice, could thus be explained in terms of the defect in post-lactational involution. There are many examples of mouse models where delayed involution has been associated with greater subsequent tumor susceptibility, due to a defect in the elimination of cell populations susceptible to transformation.[66] Remarkably, in the transgenic mouse model used in this work,[16] a specific defect in elimination during the involution of tumor cells that form *in situ* carcinomas, but normal elimination of mammary cells surrounding tumoral ones have been reported. [67] This indicates that the already fully-transformed cells may not be eliminated easily after post-lactational involution. Although there were more ERBB2-positive cells in the mammary glands of parous *Snai2 KO*$^{ERBB2+}$ mice than in the *Snai2 WT*$^{ERBB2+}$ animals at 30 days post-lactational involution, both showed the same capacity to generate mammospheres (Figure 4d). This would suggest the same number of target stem cells, in agreement with the fact that there were no differences in terms of latency and tumor numbers.

It has been reported that overexpression of activated AKT1 leads to short tumor latency in *MMTV-ErbB2* transgenic mice.[50] Here, we report that the mammary glands from parous *Snai2* KO^{ERBB2+} mice exhibited higher levels of pAKT1 than parous *Snai2* WT^{ERBB2+} mice, which could explain the tumor latency compensation seen after pregnancy (Figure 2a). Moreover, this increase in pAKT1 levels could contribute to the observed delay in mammary gland involution,[45, 46] which could lead to more target cells becoming available. pAKT1 levels would be increased by pSTAT3 through the regulation of PI3K, modifying the levels of some regulatory subunits;[46] as reported in a recent paper, this could also be performed directly by SNAI2 in colon cancer cells.[68]

In conclusion, we have demonstrated that SNAI2, although not expressed in the tumors, is important for the pathogenesis of breast cancer of luminal origin. This demonstrates the usefulness of SNAI2 inhibition for therapy or prevention in luminal breast cancer and for preventing metastasis. We also found that tumors from parous *Snai2* KO^{ERBB2+} mice had higher levels of total and phosphorylated AKT1, suggesting that this alteration in AKT1 levels would be exerted by a non-cell autonomous mechanism. It remains to be clarified how SNAI2 deficiency in other local or long-distant compartments might also contribute to the pathogenesis of luminal breast cancer. Finally, the connection observed here, as in other models, between a defect in mammary remodeling and increased susceptibility to breast cancer highlights the possibility of modifying this physiological process to develop preventive strategies against breast cancer.[66]

Materials and Methods

Animals

All mice were housed at the Animal Research Facility of the University of Salamanca. All practices were accepted by the Institutional Animal Care and Bioethical Committee of the University of Salamanca. FVB/N-Tg(MMTVneu)202Mul/J, which are FVB mice carrying the *ErbB2* protooncogene under the control of the Mouse Mammary Tumor Virus (MMTV) 3′promoter,[16] were obtained from the Jackson Laboratory (Bar Harbor, ME, USA), and wild-type (WT) FVB/N mice were purchased from Charles River (Wilmington, MA, USA). B6;129S1-*Snai2*^{tm2Grid}/J *Snai2*-deficient mice were generated by Dr. Gridley (Scarborough, ME, USA).[18] Mice were weaned at 3-4 weeks of age and analyzed for the presence of the *ErbB2* transgene. The initial F1-*Snai2*-deficient mice were generated by mating C57BL/6 *Snai2* KO males with *MMTV-ErbB2* transgenic females in a FVB genetic background. To avoid the C57BL/6-resistance effect in breast cancer development,[19-21] F1 transgene-positive/*Snai2*-deficient males were backcrossed with FVB females to obtain the F4 generation with a 90% FVB genetic background;[72] mice were intercrossed to obtain *Snai2* WT^{ERBB2+} and *Snai2* KO^{ERBB2+} Because *Snai2* KO mice are born at lower than the expected frequency and show perinatal mortality, only those KO mice that surpassed five weeks of life were included in the experiments. To generate the parous cohort, *Snai2* WT $^{ERBB2+}$ and *Snai2* KO^{ERBB2+} female mice were bred twice, and after the second lactation the cohort was followed for mammary tumor formation. All mice were maintained in ventilated filter cages under SPF conditions and were fed *ad libitum*. We estimated the number of mice based on Statgraphics Centurion software (Statpoint Technologies, Warrenton, VA, USA); thus, a minimum of total sample size of 23 animals per group was necessary to provide a 90% chance of detecting difference ≥ 1.5 standard deviations between the two populations means with 95% confidence. Taking this into account, we adapted the sample size based on the results of our previous study.[27] The usual mammary gland studies were performed in mice after a single pregnancy and lactation. All analyses were performed by certified pathologists (M.C. from the CNIO and an additional pathologist from the Comparative Pathology Core Facility) blinded to sample identity.

Protein analyses

The epithelial mammary gland component (organoids) and tumors were collected at necropsy, snap-frozen in liquid nitrogen and kept at -80 °C. Proteins were extracted from frozen tissues. Ceramic beads (Precellys, Bertin Technologies, #03961-1-009, Montigny le Bretonneux, France) were added to tissues (10-50 mg) and these were homogenized for 10 seconds, 5.5 m/s (twice), using the FastPrep Homogenizer (Thermo Savant, Thermo Fisher Scientific Inc., Waltham, MA, USA) in RIPA buffer (150 mM NaCl, 1% (v/v) NP40, 50 mM Tris-HCl at pH 8.0, 0.1% (v/v) SDS, 1 mM EDTA, 0.5% (w/v) Deoxycholate) containing cocktails of protease and phosphatase inhibitors (Roche, Basel, Switzerland) for tumors and organoids. Samples were incubated for 20 minutes on ice and centrifuged for 10 min at 13000 r.p.m. and 4°C. Supernatants were collected and quantified using the BCA Protein Assay Kit (Thermo Fisher Scientific Inc.,catalog number 23228, Waltham, MA, USA). Equivalent amounts of proteins were resolved by SDS-PAGE, and transferred to polyvinylidene difluoride membranes (Immobilon-P, Millipore, Darmstadt, Germany).

Immunoblotting was performed using the following primary antibodies: anti-phospho-AKT(Ser473) (D9E, #3787), anti-AKT (11E7, #4685), anti-AKT1 (2H10, #2967), anti-SNAI2 (#9585), anti-pSTAT3(Y705) (#9145) from Cell Signaling (Danvers, MA, USA); anti-ERBB2 (ab2428), anti-phospho-ERBB2(Tyr1248) (ab47755) from Abcam (Cambridge, United Kingdom); anti-TUBULIN (DM1A, #T6199, Sigma, St Louis,MO, USA), anti-ACTIN (C4, sc-47778, Santa Cruz, Dallas, TX, USA), anti-GAPDH (sc-25778, Santa Cruz, Dallas, TX, USA), and anti-CYCLIN D1 (C-20, sc-717, Santa Cruz, Dallas, TX, USA), anti-Estrogen Receptor alpha (ab39642, Abcam, Cambridge, United Kingdom) and subsequently with horseradish peroxidase-conjugated anti-mouse, anti-rabbit or anti-goat secondary antibodies (1:10000 dilution) (BIO-RAD, Berkeley, CA, USA), and visualized by enhanced chemiluminescence (Thermo Scientific). A total amount of protein of 100 μg from the organoids was assayed for active CASPASE-3 using the fluorometric CASPASE 3 Assay Kit (ab39383, Abcam) according to the manufacturer's instructions. For ELISA assays, the levels of phosphorylated and total AKT1 were measured using Sandwich ELISA Kits (#7142 and #7143, respectively, PathScan, Cell Signaling).

Mammary cell preparation and culture

Mammary glands were dissected out from female mice at the ages specified along the manuscript. After mechanical dissociation with two scalpels (Swann-Morton, #0511, Sheffield, United Kingdom), the tissue was placed in culture medium (DMEM/F12, 10% FBS, 1% penicillin/streptomycin, 1% Glutamine) containing 600 units/ml collagenase (Sigma, C2674, St Louis, MO, USA) and 200 units/ml hyaluronidase (Sigma, H3506, St Louis, MO, USA) and digested for 3 hours at 37° C for the mammosphere protocol, and 6 hours for FACS analysis. Organoid suspensions were obtained by differential centrifugation.[69] Mammosphere formation was achieved as previously described[70] with the following modifications: 10000 cells were seeded per well in triplicate on ultralow attachment plates (Corning, #3471, Corning, NY, USA), and after 7 days of culture only mammospheres with a diameter greater than 50 μm were counted. The mammosphere medium was prepared as previously described.[71]

X-Gal staining

For whole mount X-gal staining, *Snai2* KO^{ERBB2+} mice, which carry the *LacZ* gene in the *Snai2* locus, [18] and *Snai2* WT^{ERBB2+} mice were sacrificed and the fourth mammary gland or tumor samples were harvested and processed with the β-Galactosidase Staining kit according to the manufacturer's instructions (#9866 Cell Signaling Technology).

Mammary gland whole-mounts

The fourth (abdominal) mammary glands were removed surgically, stretched onto a glass slide and fixed with Carnoy's fixative (ethanol / chloroform / glacial acetic acid, at proportions 6/3/1, respectively) for 24 hours at room temperature. Then, they were rehydrated with a graded series of ethanol solutions, washed for 5 minutes in distilled water and stained overnight in alum carmine solution (Sigma, C1022). The following day, the mammary glands were dehydrated with a graded series of ethanol solutions. Mammary glands were cleared in xylene until the fat had been sufficiently removed from the glands.

Images were analyzed using ImageJ software (National Institutes of Health, Bethesda, MD, USA).

Immunostaining

Mammary glands or tumors were fixed in 4% paraformaldehyde overnight at room temperature and washed in 70% EtOH before paraffin inclusion. Sections of 3 μm were deparaffinized and processed for antigen retrieval by incubation in a microwave with citrate buffer (pH 6) for cleaved CASPASE-3 and ERBB2, but at pH 8 for pSTAT3. The primary antibodies were incubated using the Ventana Discovery automated immunohistochemistry research slide-staining system (Tucson, AZ85755) with the following antibody dilutions: 1/50 Ki-67 (MAD020310Q, Master Diagnostica, Granada, Spain), 1/50 cleaved CASPASE-3(Asp175) (#9662, Cell Signaling), 1/75 ERBB2 (ab2438, Abcam), 1/50 pSTAT3(Y705) (D3A7, #9145, Cell Signaling), 1/50 CK6 (SPM269, ab75703, Abcam), 1/100 CK8 (ab59400, Abcam) and 1/100 Progesterone Receptor (Y85, MAD210302Q, Master Diagnostica). Ki-67-, CASPASE-3- and ERBB2-positive cells from tumors were quantified with the ARIOL software at the Centro Nacional de Investigaciones Oncológicas (CNIO, Madrid, Spain). To accomplish this, tumors from *Snai2* WT^{ERBB2} and *Snai2* KO^{ERBB2} nulliparous and parous mice (10 tumors from each group) were stained in triplicate on tissue-array sections.

Cell culture and retroviral infection

The HC11 cell line was obtained from Dr. Montoliú (Centro Nacional de Biotecnología, Spain) in February 2014. Experiments were performed during the ensuing 3 months. The cells showed the correct phenotype, with the expected morphology and growth curves; and were previously tested for mycoplasma contamination. HC11 cells were cultured with RPMI-1640 medium with 10% heat-inactivated FCS, 5 μg/ml insulin, 20 ng/ml epidermal growth factor, and 1% penicillin-streptomycin. HC11 cells were infected with retrovirus carrying *Snai2* shRNA or a control.[72] Recombinant retroviruses were produced from Phoenix-A cells, which were transiently transfected with plasmid DNA (shRNA *Snai2*) using LT-1 reagents (Mirus, Madison, WI, USA). HC11 cells were infected in the presence of polybrene (30 μg/ml). Two days later, the medium was replaced with fresh virus-containing medium and the cells were allowed to grow to confluence for three days in the presence or absence of prolactin at 5 μg/ml or progesterone at 10^{-8} M (Sigma).

Statistical analyses

Mammary tumor latency, disease duration and lifespans were compared in the *Snai2* WT^{ERBB2+} and *Snai2* KO^{ERBB2+} female mice using the Kaplan-Meier estimator and the Log-Rank test. The number of tumors, the number of lung metastases and other determinations were evaluated with the Mann-Whitney U test for two groups, and with the Kruskal-Wallis test more than two groups, followed by Dunn's multiple comparison post-test. Incidence and multiplicity were evaluated using Fisher's exact tests. For all analyses, *P* values ≤ 0.05 were considered statistically significant. The analyses were performed using the SPSS (IBM, Armonk, NY, USA) and JMP/SAS (SAS Institute, Cary, NC, USA) statistical packages.

Supplementary Material

Refer to Web version on PubMed Central for supplementary material.

Acknowledgments

JPL was partially supported by FEDER and MICINN (PLE2009-119, SAF2014-56989-R), Instituto de Salud Carlos III (PI07/0057, PI10/00328, PIE14/00066), Junta de Castilla y León (SAN673/SA26/08, SAN126/SA66/09, SA078A09, CSI034U13), the "Fundación Eugenio Rodríguez Pascual", the "Fundación Inbiomed" (Instituto Oncológico Obra Social de la Caja Guipozcoa-San Sebastian, Kutxa), and the "Fundación Sandra Ibarra de Solidaridad frente al Cáncer". AC was supported by FIS (PI07/0057) and MICINN (PLE2009-119). SCLL was funded by a JAEdoc Fellowship (CSIC)/FSE. MMSF and ABG are funded by fellowships from the Junta de Castilla y Leon. JHM was supported by the National Institutes of Health, a National Cancer Institute grant (R01 CA116481), and the Low-Dose Scientific Focus Area, Office of Biological & Environmental Research, US Department of Energy (DE-AC02-05CH11231). We thank Dr. Montoliú for HC11 cells, Dr. García Macías and the Comparative Pathology Core Facility of the "Centro de Investigación del Cáncer (CIC) de la Universidad de Salamanca" for Pathology support, María Luz Hernández Mulas and Isabel Ramos for technical assistance, Dr. Sánchez-García and Dr. Martin-Zanca for useful comments along this project, Dr. Balmain and Dr. Lazo for comments about the manuscript, and Nicholas Skinner for his useful help in English editing.

References

1. Perou CM, Sorlie T, Eisen MB, van de Rijn M, Jeffrey SS, Rees CA, et al. Molecular portraits of human breast tumours. Nature. 2000; 406:747–752. [PubMed: 10963602]
2. Slamon DJ, Godolphin W, Jones LA, Holt JA, Wong SG, Keith DE, et al. Studies of the HER-2/neu proto-oncogene in human breast and ovarian cancer. Science. 1989; 244:707–712. [PubMed: 2470152]
3. Hajra KM, Chen DY, Fearon ER. The SLUG zinc-finger protein represses E-cadherin in breast cancer. Cancer research. 2002; 62:1613–1618. [PubMed: 11912130]
4. Barrallo-Gimeno A, Nieto MA. The Snail genes as inducers of cell movement and survival: implications in development and cancer. Development. 2005; 132:3151–3161. [PubMed: 15983400]
5. Inukai T, Inoue A, Kurosawa H, Goi K, Shinjyo T, Ozawa K, et al. SLUG, a ces-1-related zinc finger transcription factor gene with antiapoptotic activity, is a downstream target of the E2A-HLF oncoprotein. Molecular cell. 1999; 4:343–352. [PubMed: 10518215]
6. Perez-Mancera PA, Gonzalez-Herrero I, Perez-Caro M, Gutierrez-Cianca N, Flores T, Gutierrez-Adan A, et al. SLUG in cancer development. Oncogene. 2005; 24:3073–3082. [PubMed: 15735690]
7. Wu WS, Heinrichs S, Xu D, Garrison SP, Zambetti GP, Adams JM, et al. Slug antagonizes p53-mediated apoptosis of hematopoietic progenitors by repressing puma. Cell. 2005; 123:641–653. [PubMed: 16286009]
8. Nieto MA. The snail superfamily of zinc-finger transcription factors. Nature reviews Molecular cell biology. 2002; 3:155–166. [PubMed: 11994736]
9. Nassour M, Idoux-Gillet Y, Selmi A, Come C, Faraldo ML, Deugnier MA, et al. Slug controls stem/progenitor cell growth dynamics during mammary gland morphogenesis. PloS one. 2012; 7:e53498. [PubMed: 23300933]
10. Guo W, Keckesova Z, Donaher JL, Shibue T, Tischler V, Reinhardt F, et al. Slug and Sox9 cooperatively determine the mammary stem cell state. Cell. 2012; 148:1015–1028. [PubMed: 22385965]
11. Cobaleda C, Perez-Caro M, Vicente-Duenas C, Sanchez-Garcia I. Function of the zinc-finger transcription factor SNAI2 in cancer and development. Annual review of genetics. 2007; 41:41–61.
12. Storci G, Sansone P, Trere D, Tavolari S, Taffurelli M, Ceccarelli C, et al. The basal-like breast carcinoma phenotype is regulated by SLUG gene expression. The Journal of pathology. 2008; 214:25–37. [PubMed: 17973239]
13. Proia TA, Keller PJ, Gupta PB, Klebba I, Jones AD, Sedic M, et al. Genetic predisposition directs breast cancer phenotype by dictating progenitor cell fate. Cell stem cell. 2011; 8:149–163. [PubMed: 21295272]

14. Neve RM, Chin K, Fridlyand J, Yeh J, Baehner FL, Fevr T, et al. A collection of breast cancer cell lines for the study of functionally distinct cancer subtypes. Cancer cell. 2006; 10:515–527. [PubMed: 17157791]
15. Come C, Magnino F, Bibeau F, De Santa Barbara P, Becker KF, Theillet C, et al. Snail and slug play distinct roles during breast carcinoma progression. Clinical cancer research : an official journal of the American Association for Cancer Research. 2006; 12:5395–5402. [PubMed: 17000672]
16. Guy CT, Webster MA, Schaller M, Parsons TJ, Cardiff RD, Muller WJ. Expression of the neu protooncogene in the mammary epithelium of transgenic mice induces metastatic disease. Proceedings of the National Academy of Sciences of the United States of America. 1992; 89:10578–10582. [PubMed: 1359541]
17. Herschkowitz JI, Simin K, Weigman VJ, Mikaelian I, Usary J, Hu Z, et al. Identification of conserved gene expression features between murine mammary carcinoma models and human breast tumors. Genome biology. 2007; 8:R76. [PubMed: 17493263]
18. Jiang R, Lan Y, Norton CR, Sundberg JP, Gridley T. The Slug gene is not essential for mesoderm or neural crest development in mice. Developmental biology. 1998; 198:277–285. [PubMed: 9659933]
19. Rowse GJ, Ritland SR, Gendler SJ. Genetic modulation of neu proto-oncogene-induced mammary tumorigenesis. Cancer research. 1998; 58:2675–2679. [PubMed: 9635596]
20. Ullrich RL, Bowles ND, Satterfield LC, Davis CM. Strain-dependent susceptibility to radiation-induced mammary cancer is a result of differences in epithelial cell sensitivity to transformation. Radiation research. 1996; 146:353–355. [PubMed: 8752316]
21. Davie SA, Maglione JE, Manner CK, Young D, Cardiff RD, MacLeod CL, et al. Effects of FVB/NJ and C57Bl/6J strain backgrounds on mammary tumor phenotype in inducible nitric oxide synthase deficient mice. Transgenic research. 2007; 16:193–201. [PubMed: 17206489]
22. Markel P, Shu P, Ebeling C, Carlson GA, Nagle DL, Smutko JS, et al. Theoretical and empirical issues for marker-assisted breeding of congenic mouse strains. Nature genetics. 1997; 17:280–284. [PubMed: 9354790]
23. Sanchez-Garcia I. The crossroads of oncogenesis and metastasis. The New England journal of medicine. 2009; 360:297–299. [PubMed: 19144947]
24. Liu JC, Deng T, Lehal RS, Kim J, Zacksenhaus E. Identification of tumorsphere- and tumor-initiating cells in HER2/Neu-induced mammary tumors. Cancer research. 2007; 67:8671–8681. [PubMed: 17875707]
25. Gunzburg WH, Salmons B. Factors controlling the expression of mouse mammary tumour virus. The Biochemical journal. 1992; 283(Pt 3):625–632. [PubMed: 1317161]
26. Landis MD, Seachrist DD, Abdul-Karim FW, Keri RA. Sustained trophism of the mammary gland is sufficient to accelerate and synchronize development of ErbB2/Neu-induced tumors. Oncogene. 2006; 25:3325–3334. [PubMed: 16434967]
27. Castellanos-Martín A, CL S, Sáez-Freire M, Blanco-Gómez A, Hontecillas-Prieto L, Patino-Alonso C, Galindo-Villardon P, Pérez del Villar L, Martín-Seisdedos C, Isidoro-Garcia M, Abad-Hernández M, Cruz-Hernández JJ, Rodríguez-Sánchez CA, González-Sarmiento R, Alonso-López D, de las Rivas J, García-Cenador Begoña, García-Criado J, Lee DY, Bowen B, Reindl W, Northen T, Mao JH, Pérez-Losada J. Unraveling Heterogeneous Susceptibility and the Evolution of Breast Cancer by a Systems Biology Approach. Genome Biology. 2015; 16:14. [PubMed: 25616342]
28. Knight CH, Peaker M. Development of the mammary gland. Journal of reproduction and fertility. 1982; 65:521–536. [PubMed: 7097655]
29. Mukherjee S, Louie SG, Campbell M, Esserman L, Shyamala G. Ductal growth is impeded in mammary glands of C-neu transgenic mice. Oncogene. 2000; 19:5982–5987. [PubMed: 11146549]
30. Perez-Losada J, Balmain A. Stem-cell hierarchy in skin cancer. Nature reviews Cancer. 2003; 3:434–443. [PubMed: 12778133]

31. Shackleton M, Vaillant F, Simpson KJ, Stingl J, Smyth GK, Asselin-Labat ML, et al. Generation of a functional mammary gland from a single stem cell. Nature. 2006; 439:84–88. [PubMed: 16397499]
32. Dontu G, Abdallah WM, Foley JM, Jackson KW, Clarke MF, Kawamura MJ, et al. In vitro propagation and transcriptional profiling of human mammary stem/progenitor cells. Genes & development. 2003; 17:1253–1270. [PubMed: 12756227]
33. Mani SA, Guo W, Liao MJ, Eaton EN, Ayyanan A, Zhou AY, et al. The epithelial-mesenchymal transition generates cells with properties of stem cells. Cell. 2008; 133:704–715. [PubMed: 18485877]
34. Phillips S, Prat A, Sedic M, Proia T, Wronski A, Mazumdar S, et al. Cell-State Transitions Regulated by SLUG Are Critical for Tissue Regeneration and Tumor Initiation. Stem cell reports. 2014; 2:633–647. [PubMed: 24936451]
35. Stingl J, Eirew P, Ricketson I, Shackleton M, Vaillant F, Choi D, et al. Purification and unique properties of mammary epithelial stem cells. Nature. 2006; 439:993–997. [PubMed: 16395311]
36. Welm BE, Tepera SB, Venezia T, Graubert TA, Rosen JM, Goodell MA. Sca-1(pos) cells in the mouse mammary gland represent an enriched progenitor cell population. Developmental biology. 2002; 245:42–56. [PubMed: 11969254]
37. Deugnier MA, Faraldo MM, Teuliere J, Thiery JP, Medina D, Glukhova MA. Isolation of mouse mammary epithelial progenitor cells with basal characteristics from the Comma-Dbeta cell line. Developmental biology. 2006; 293:414–425. [PubMed: 16545360]
38. Lo PK, Kanojia D, Liu X, Singh UP, Berger FG, Wang Q, et al. CD49f and CD61 identify Her2/neu-induced mammary tumor-initiating cells that are potentially derived from luminal progenitors and maintained by the integrin-TGFbeta signaling. Oncogene. 2012; 31:2614–2626. [PubMed: 21996747]
39. Little JL, Serzhanova V, Izumchenko E, Egleston BL, Parise E, Klein-Szanto AJ, et al. A requirement for Nedd9 in luminal progenitor cells prior to mammary tumorigenesis in MMTV-HER2/ErbB2 mice. Oncogene. 2014; 33:411–420. [PubMed: 23318423]
40. Shehata M, Teschendorff A, Sharp G, Novcic N, Russell IA, Avril S, et al. Phenotypic and functional characterisation of the luminal cell hierarchy of the mammary gland. Breast cancer research : BCR. 2012; 14:R134. [PubMed: 23088371]
41. Prater MD, Petit V, Alasdair Russell I, Giraddi RR, Shehata M, Menon S, et al. Mammary stem cells have myoepithelial cell properties. Nature cell biology. 2014; 16:942–950. 941–947. [PubMed: 25173976]
42. Watson CJ, Kreuzaler PA. Remodeling mechanisms of the mammary gland during involution. The International journal of developmental biology. 2011; 55:757–762. [PubMed: 22161832]
43. Cardiff RD, Wellings SR. The comparative pathology of human and mouse mammary glands. Journal of mammary gland biology and neoplasia. 1999; 4:105–122. [PubMed: 10219910]
44. Chapman RS, Lourenco PC, Tonner E, Flint DJ, Selbert S, Takeda K, et al. Suppression of epithelial apoptosis and delayed mammary gland involution in mice with a conditional knockout of Stat3. Genes & development. 1999; 13:2604–2616. [PubMed: 10521404]
45. Schwertfeger KL, Richert MM, Anderson SM. Mammary gland involution is delayed by activated Akt in transgenic mice. Molecular endocrinology. 2001; 15:867–881. [PubMed: 11376107]
46. Abell K, Bilancio A, Clarkson RW, Tiffen PG, Altaparmakov AI, Burdon TG, et al. Stat3-induced apoptosis requires a molecular switch in PI(3)K subunit composition. Nature cell biology. 2005; 7:392–398. [PubMed: 15793565]
47. Berclaz G, Altermatt HJ, Rohrbach V, Siragusa A, Dreher E, Smith PD. EGFR dependent expression of STAT3 (but not STAT1) in breast cancer. International journal of oncology. 2001; 19:1155–1160. [PubMed: 11713584]
48. Diaz N, Minton S, Cox C, Bowman T, Gritsko T, Garcia R, et al. Activation of stat3 in primary tumors from high-risk breast cancer patients is associated with elevated levels of activated SRC and survivin expression. Clinical cancer research : an official journal of the American Association for Cancer Research. 2006; 12:20–28. [PubMed: 16397019]

49. Humphreys RC, Rosen JM. Stably transfected HC11 cells provide an in vitro and in vivo model system for studying Wnt gene function. Cell growth & differentiation : the molecular biology journal of the American Association for Cancer Research. 1997; 8:839–849. [PubMed: 9269893]
50. Hutchinson JN, Jin J, Cardiff RD, Woodgett JR, Muller WJ. Activation of Akt-1 (PKB-alpha) can accelerate ErbB-2-mediated mammary tumorigenesis but suppresses tumor invasion. Cancer research. 2004; 64:3171–3178. [PubMed: 15126356]
51. Dillon RL, Muller WJ. Distinct biological roles for the akt family in mammary tumor progression. Cancer research. 2010; 70:4260–4264. [PubMed: 20424120]
52. Villarejo A, Molina-Ortiz P, Montenegro Y, Moreno-Bueno G, Morales S, Santos V, et al. Loss of Snail2 favors skin tumor progression by promoting the recruitment of myeloid progenitors. Carcinogenesis. 2015
53. Cheung KJ, Gabrielson E, Werb Z, Ewald AJ. Collective invasion in breast cancer requires a conserved basal epithelial program. Cell. 2013; 155:1639–1651. [PubMed: 24332913]
54. Carpenter RL, Paw I, Dewhirst MW, Lo HW. Akt phosphorylates and activates HSF-1 independent of heat shock, leading to Slug overexpression and epithelial-mesenchymal transition (EMT) of HER2-overexpressing breast cancer cells. Oncogene. 2014
55. Hudson LG, Choi C, Newkirk KM, Parkhani J, Cooper KL, Lu P, et al. Ultraviolet radiation stimulates expression of Snail family transcription factors in keratinocytes. Molecular carcinogenesis. 2007; 46:257–268. [PubMed: 17295233]
56. Mittal MK, Singh K, Misra S, Chaudhuri G. SLUG-induced elevation of D1 cyclin in breast cancer cells through the inhibition of its ubiquitination. The Journal of biological chemistry. 2011; 286:469–479. [PubMed: 21044962]
57. Bowe DB, Kenney NJ, Adereth Y, Maroulakou IG. Suppression of Neu-induced mammary tumor growth in cyclin D1 deficient mice is compensated for by cyclin E. Oncogene. 2002; 21:291–298. [PubMed: 11803472]
58. Muraoka RS, Lenferink AE, Law B, Hamilton E, Brantley DM, Roebuck LR, et al. ErbB2/Neu-induced, cyclin D1-dependent transformation is accelerated in p27-haploinsufficient mammary epithelial cells but impaired in p27-null cells. Molecular and cellular biology. 2002; 22:2204–2219. [PubMed: 11884607]
59. Van Duuren BL, Sivak A, Katz C, Seidman I, Melchionne S. The effect of aging and interval between primary and secondary treatment in two-stage carcinogenesis on mouse skin. Cancer research. 1975; 35:502–505. [PubMed: 1116119]
60. Manzanares M, Locascio A, Nieto MA. The increasing complexity of the Snail gene superfamily in metazoan evolution. Trends in genetics : TIG. 2001; 17:178–181. [PubMed: 11275308]
61. Hinohara K, Kobayashi S, Kanauchi H, Shimizu S, Nishioka K, Tsuji E, et al. ErbB receptor tyrosine kinase/NF-kappaB signaling controls mammosphere formation in human breast cancer. Proceedings of the National Academy of Sciences of the United States of America. 2012; 109:6584–6589. [PubMed: 22492965]
62. Zhang W, Tan W, Wu X, Poustovoitov M, Strasner A, Li W, et al. A NIK-IKKalpha module expands ErbB2-induced tumor-initiating cells by stimulating nuclear export of p27/Kip1. Cancer cell. 2013; 23:647–659. [PubMed: 23602409]
63. Korkaya H, Paulson A, Iovino F, Wicha MS. HER2 regulates the mammary stem/progenitor cell population driving tumorigenesis and invasion. Oncogene. 2008; 27:6120–6130. [PubMed: 18591932]
64. Cao Y, Luo JL, Karin M. IkappaB kinase alpha kinase activity is required for self-renewal of ErbB2/Her2-transformed mammary tumor-initiating cells. Proceedings of the National Academy of Sciences of the United States of America. 2007; 104:15852–15857. [PubMed: 17890319]
65. Jeselsohn R, Brown NE, Arendt L, Klebba I, Hu MG, Kuperwasser C, et al. Cyclin D1 kinase activity is required for the self-renewal of mammary stem and progenitor cells that are targets of MMTV-ErbB2 tumorigenesis. Cancer cell. 2010; 17:65–76. [PubMed: 20129248]
66. Radisky DC, Hartmann LC. Mammary involution and breast cancer risk: transgenic models and clinical studies. Journal of mammary gland biology and neoplasia. 2009; 14:181–191. [PubMed: 19404726]

67. Lazar H, Baltzer A, Gimmi C, Marti A, Jaggi R. Over-expression of erbB-2/neu is paralleled by inhibition of mouse-mammary-epithelial-cell differentiation and developmental apoptosis. International journal of cancer Journal international du cancer. 2000; 85:578–583. [PubMed: 10699933]

68. Wang G, Yang X, Li C, Cao X, Luo X, Hu J. PIK3R3 induces epithelial-to-mesenchymal transition and promotes metastasis in colorectal cancer. Molecular cancer therapeutics. 2014; 13:1837–1847. [PubMed: 24837077]

69. Kuperwasser C, Chavarria T, Wu M, Magrane G, Gray JW, Carey L, et al. Reconstruction of functionally normal and malignant human breast tissues in mice. Proceedings of the National Academy of Sciences of the United States of America. 2004; 101:4966–4971. [PubMed: 15051869]

70. Shaw FL, Harrison H, Spence K, Ablett MP, Simoes BM, Farnie G, et al. A detailed mammosphere assay protocol for the quantification of breast stem cell activity. Journal of mammary gland biology and neoplasia. 2012; 17:111–117. [PubMed: 22665270]

71. Cicalese A, Bonizzi G, Pasi CE, Faretta M, Ronzoni S, Giulini B, et al. The tumor suppressor p53 regulates polarity of self-renewing divisions in mammary stem cells. Cell. 2009; 138:1083–1095. [PubMed: 19766563]

72. Ventura A, Meissner A, Dillon CP, McManus M, Sharp PA, Van Parijs L, et al. Cre-lox-regulated conditional RNA interference from transgenes. Proceedings of the National Academy of Sciences of the United States of America. 2004; 101:10380–10385. [PubMed: 15240889]

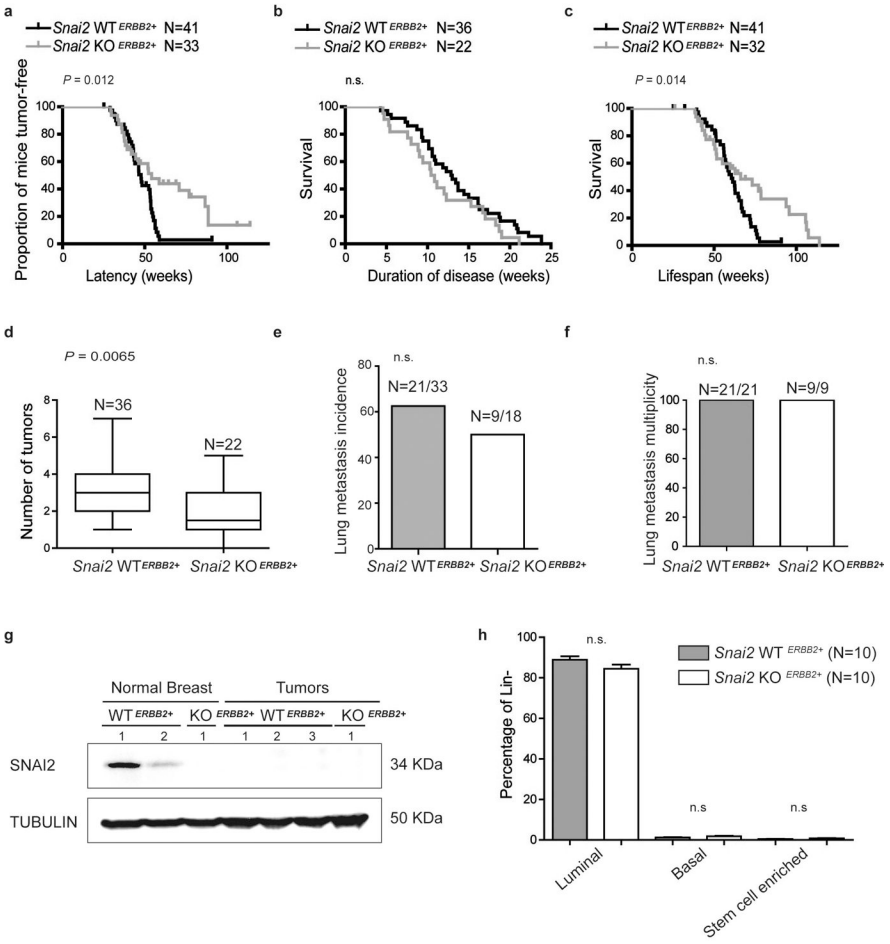

Figure 1. SNAI2 participates in the early stages of luminal breast cancer development

Comparison of different tumor pathophenotypes in nulliparous female mice: (**a**) Latency. (**b**) Duration of disease. (**c**) Survival. (**d**) Number of tumors. (**e**) Incidence of metastases. (**f**) Multiplicity of metastases. (**g**) Detection of SNAI2 in mammary glands and luminal tumors (western blot). (**h**) Comparison between tumors from *Snai*2 WT $^{ERBB2+}$ and *Snai2* KO^{ERBB2+} mice of the percentage of viable Lin- cells corresponding to the luminal lineage (CD24^{hi} CD29^{lo}), basal lineage (CD24^{lo} CD29^{hi}), and the stem-cell-enriched population (CD24^{lo} CD29^{hi} CD49f^{hi}).

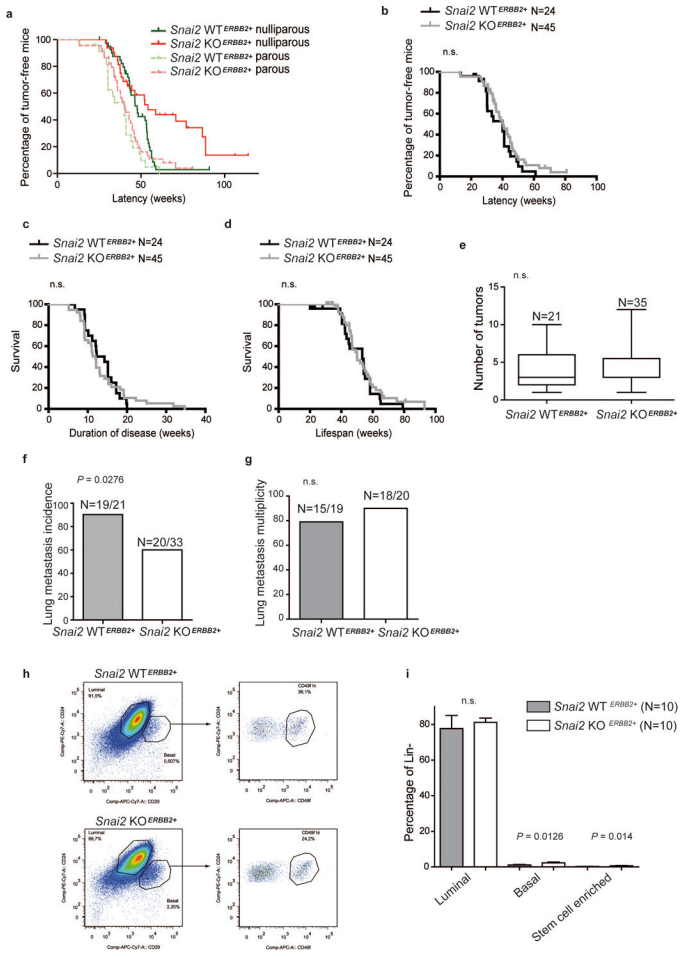

Figure 2. Effect of pregnancy in breast cancer development under *Snai2* deficiency

(**a**) Tumor latency in nulliparous and parous mice. Note that *Snai2* KO^{ERBB2+} mice showed the greatest shortening of tumor latency after pregnancy. (**b**-**h**) Comparison of different tumor pathophenotypes in parous female mice: (**b**) latency; (**c**) duration of disease; (**d**) lifespan; (**e**) number of tumors; (**f**) incidence of metastases; (**g**) multiplicity of metastases. (**h**) Representative dotplots of viable Lin- tumor cells from parous *Snai2* WT^{ERBB2+} (upper panel) and parous *Snai2* KO^{ERBB2+} (lower panel) mice, showing the gating strategy followed to quantify luminal, basal, and stem-cell-enriched populations. (**i**) Comparison between tumors from parous *Snai2* WT^{ERBB2+} and *Snai2* KO^{ERBB2+} mice of the percentage of viable Lin- cells corresponding to the luminal lineage (CD24^{hi} CD29^{lo}), basal lineage (CD24^{lo} CD29^{hi}), and the stem-cell-enriched population (CD24^{lo} CD29^{hi} CD49f^{hi}).

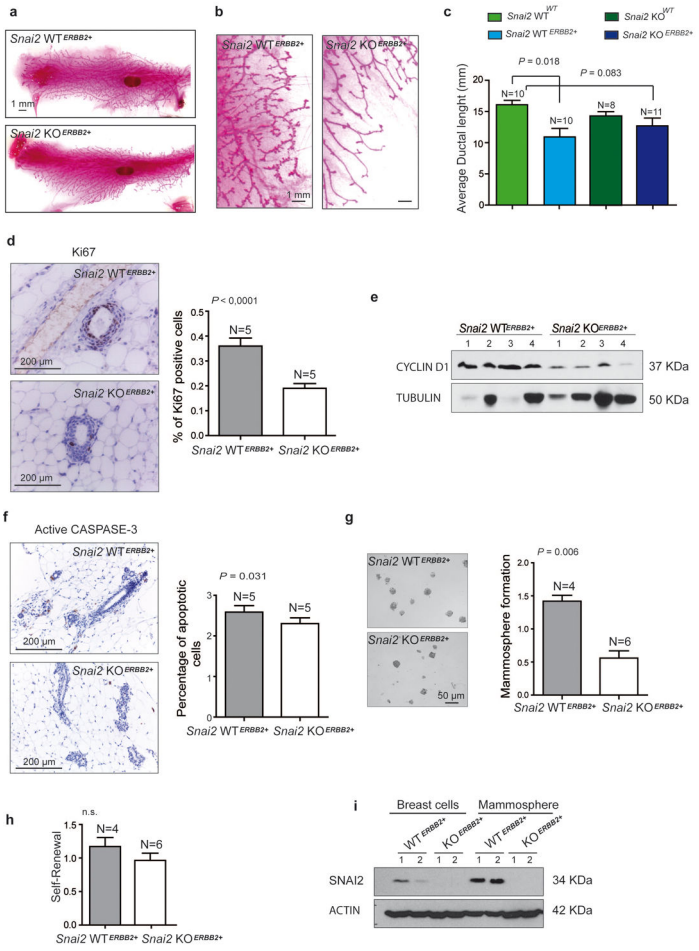

Figure 3. Mammary glands from nulliparous *Snai2* KO^{ERBB2+} mice show defects in cellular turnover and stem-cell populations

(a) Fat pad in mammary glands normally filled by ducts (whole-mount). (**b**) Defect in side branching in *Snai2* KO^{ERBB2+} mice. (**c**) Average length of primary ducts. Distances were estimated based on whole-mount preparations. (**d**) Ki67 detection in mammary glands from female mice (immunohistochemistry) (left). Percentage of Ki67-positive cells per gland determined in five different mice (right). (**e**) Detection of CYCLIN D1 in mammary glands by western blot. Each number represents an epithelial mammary gland from an individual mouse. (**f**) Cleaved CASPASE-3, in nulliparous mice (immunohistochemistry) (left). Percentage of cleaved CASPASE-3-stained cells per gland of five different mice (right). (**g**) Ability to generate mammospheres *ex vivo*. Mammospheres were obtained from the mammary glands of 6-week-old mice. (**h**) Propagating ability of mammospheres *in vitro*. (**i**) SNAI2 protein expression in epithelial mammary glands versus mammospheres obtained from the same preparation by western blot.

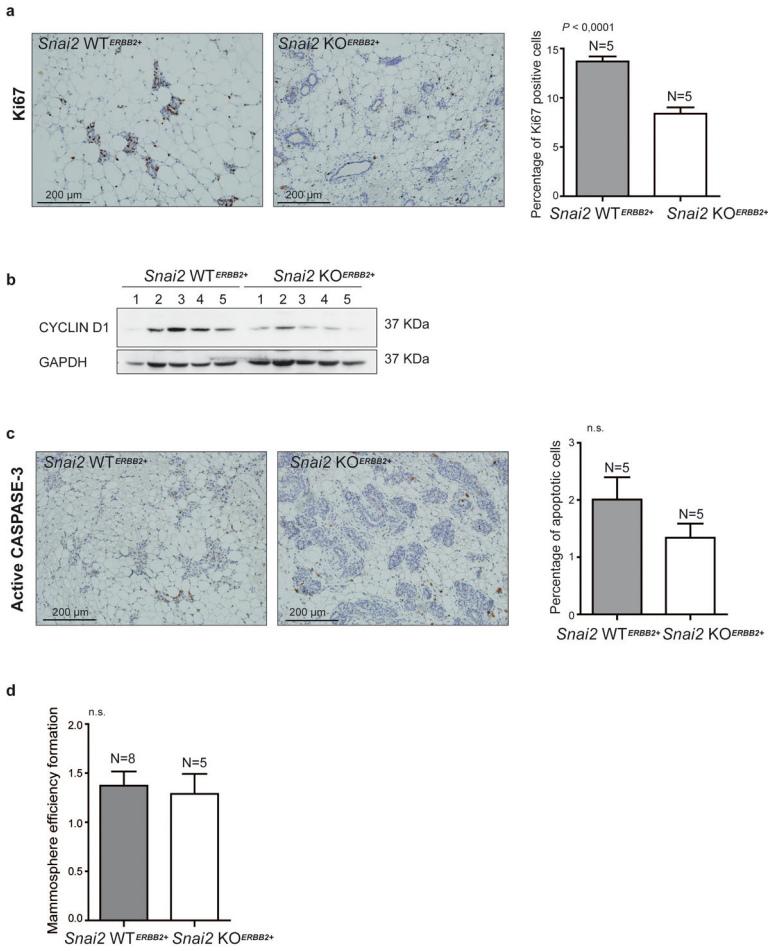

Figure 4. *Snai2* KO^{ERBB2+} mice compensate the defect in the number of mammospheres after pregnancy

All analyses from this figure were performed using parous mice at 30 days post-lactation. (**a**) Immunohistochemical staining for Ki67 (left). Percentage of Ki67-positive cells per gland (right). (**b**) Detection of CYCLIN D1 by western blot. Each number represents an epithelial mammary gland from an individual mouse. (**c**) Tissue staining against cleaved-CASPASE-3 (left). Percentage of CASPASE-3-positive cells per gland (right). (**d**) Mammosphere yield obtained from mammary glands.

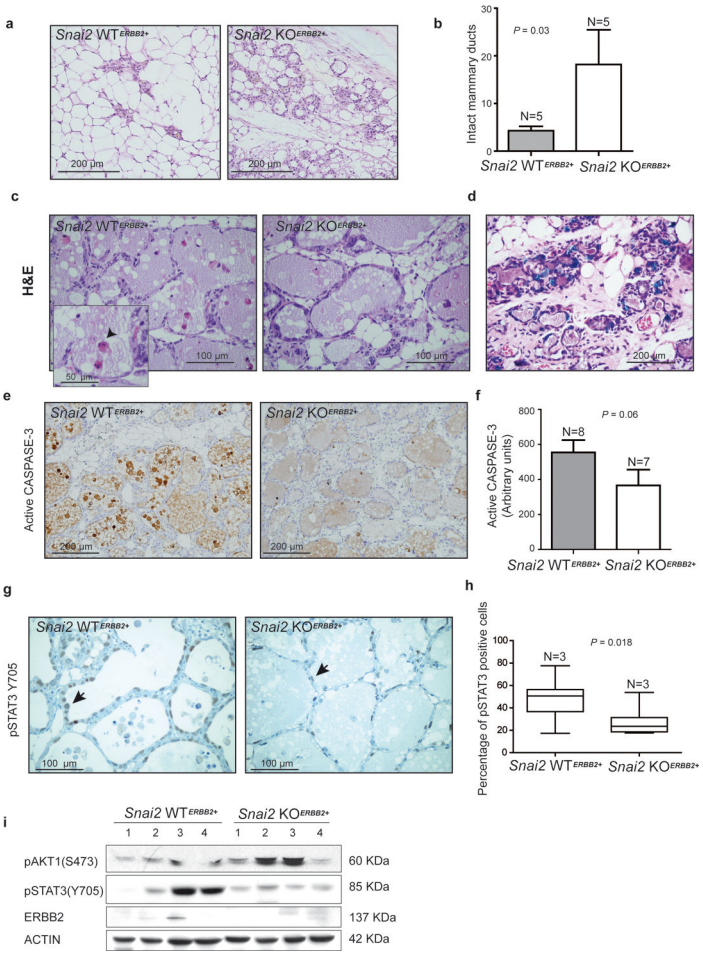

Figure 5. SNAI2 is necessary for normal mammary gland involution

(**A**) Mammary glands from parous mice at 30 days post-lactation (hematoxilin-eosin). (**b**) Quantification of intact mammary ducts: 10 fields were counted per mammary gland from five individual mice of each genotype. (**c**) Mammary glands from parous mice at three days post-lactation (hematoxilin-eosin). Arrowheads in *Snai2* WT^{ERBB2+} mice indicate an apoptotic body. (**d**) SNAI2 expression at 3 days post-lactational involution (X-Gal staining and hematoxilin-eosin). (**e**) Cleaved CASPASE-3 in mammary glands from parous female mice at 3 days post-lactation involution (immunohistochemistry). (**f**) Quantification of CASPASE-3 activity per gland from parous female mice by ELISA (fluorometric assay). (**g**) pSTAT3(Y705) in mammary glands from parous mice at 3 days post-lactation (immunohistochemistry). Arrowheads indicate positive cells. (**h**) Quantification of pSTAT3(Y705) positive cells in parous mice at three days post-lactation (10 fields were counted per gland in three different mice). (**i**) Detection of pAKT1(S473) and pSTAT3(Y705) in organoids from mammary glands at 3 days post-lactation. Each number corresponds to an individual mammary gland from four individual mice.

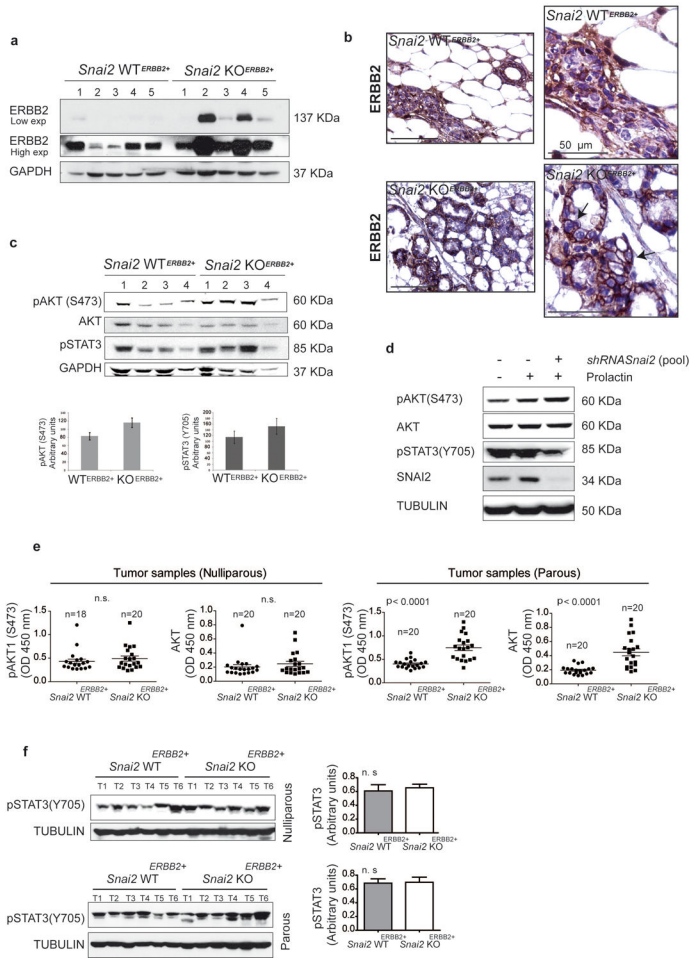

Figure 6. Downregulation of *Snai2* in HC11 cells leads to an increase in phosphorylation of AKT1 and a decrease in pSTAT3

(**a**) Detection of ERBB2 from parous mammary glands at 30 days post-lactation by western blot. Each number corresponds to an individual mammary gland from an individual mouse. (**b**) ERBB2 expression in mammary glands from parous mice at 30 days post-lactation (immunohistochemistry). Arrowheads indicate complete membrane stain-positive cells. (**c**) Detection of AKT and pSTAT3 from parous mammary glands at 30 days post-lactation by western blot. Each number corresponds to an epithelial mammary gland from an individual mouse (N = 4). pAKT and pSTAT3 bands were quantified, and normalized intensities were calculated as averages from 4 individual mice. (**d**) HC11 cells transfected with *Snai2* shRNA were treated with prolactin for three days; GFP-positive cells were sorted by flow cytometry, and AKT and pSTAT3 protein levels were assessed. (**e**) Levels of total and pAKT1 (S473) from tumor samples (ELISA). (**f**) Detection of pSTAT3 from nulliparous and parous tumors by western blot.

Table 1

Pathophenotypes studied in nulliparous and parous *Snai2* WT^{ERBB2+} and *Snai2* KO^{ERBB2+} female mice

Tumor traits were compared using the Mann Whitney U test, and the temporal stages of the disease were evaluated using the Kaplan-Meier estimator and the Log-Rank test. The incidence and multiplicity of tumors and metastases were compared with Fisher's exact test. The numbers of mice used in the experiments are shown in the respective figures along the manuscript. N: number of mice. The *N* values shown in the local growth rate represent all tumors analyzed. IR: interquartile range; n.s.: non-significant *P* values.

A. TEMPORAL STAGES			***Snai2* WT^{ERBB2+}**	***Snai2* KO^{ERBB2+}**	***P* value**
Tumor Latency (weeks)					
Latency interval (N)	*Nuliparous*		28.8-90.9 (N=41)	29.7-114 (N=33)	
	Parous		21.6-61 (N=24)	13.1-80.8 (N=45)	
Median (IR)	*Nuliparous*		47.7 (13.8)	54.1 (21.04)	0.0127
	Parous		40 (14.82)	40.4 (13.21)	n.s.
		***P* value**	0.0038	0.0004	
Duration of Disease (weeks)					
Disease interval (N)	*Nuliparous*		4.28-23.86 (N=36)	4.57-21.14 (N=22)	
	Parous		6.7-20 (N=24)	5.14-22.29 (N=45)	
Median (IR)	*Nuliparous*		12.9 (12.75)	10.36 (10.39)	n.s.
	Parous		13.3 (7.46)	11.6 (5.14)	n.s.
		***P* value**	n.s.	n.s.	
Lifespan (weeks)					
Lifespan interval (N)	*Nuliparous*		39.4-90.9 (N=41)	38.3-114 (N=32)	
	Parous		20-79.1 (N=24)	32.1-93 (N=45)	
Median (IR)	*Nuliparous*		60.42 (14.28)	66.14 (32.93)	0.0145
	Parous		53.38 (17.07)	50 (16.14)	n.s.
B. TUMOR TRAITS		***P* value**	0.0089	0.0009	
Tumor Number					
Incidence % (rate)	*Nuliparous*		87.8% (36/41)	66.67% (22/33)	0.0453
	Parous		87,5% (21/24)	76,09% (35/46)	n.s.
		***P* value**	n.s.	n.s.	
Multiplicity (2 or more)	*Nuliparous*		88.89% (32/36)	59.09% (13/22)	0.0204
	Parous		90.48% (19/21)	94.29% (33/35)	n.s.

A. TEMPORAL STAGES			***Snai2* WT^{ERBB2+}**	***Snai2* KO^{ERBB2+}**	***P* value**
		***P* value**	n.s.	0.0017	
Median (IR)	*Nuliparous*		3 (2)	1 (3)	0.0012
	Parous		3 (4)	3 (3.25)	n.s.
		***P* value**	n.s.	0.0076	
Local Growth Rate					
Median (IR) (N)	*Nuliparous*		0.32 (0.17) (N=59)	0.33 (0.136) (N=26)	n.s.
	Parous		0.24 (0.21) (N=46)	0.32 (0.27) (N=72)	n.s.
		***P* value**	n.s.	n.s.	
Metastasis					
Incidence % (rate)	*Nuliparous*		63.64% (21/33)	50% (9/18)	n.s.
	Parous		90.47% (19/21)	61% (20/33)	0.0276
		***P* value**	0.0535	n.s.	
Multiplicity (2 or more)	*Nuliparous*		100% (21/21)	100% (9/9)	n.s.
	Parous		78.9% (15/19)	90% (18/20)	n.s.
		***P* value**	0.0424	n.s.	
Median (IR)	*Nuliparous*		5 (8.5)	1 (5.25)	n.s.
	Parous		8 (18)	3 (10)	0.0349
		***P* value**	n.s.	n.s.	

Oncogene. Author manuscript; available in PMC 2016 March 03.